Semianalytical approach for the Vaidya metric in double-null coordinates

Fernando Girotto

Instituto de Física, Universidade de São Paulo, CP 66318, 05315-970 São Paulo, SP, Brazil

Alberto Saa*

Departamento de Matemática Aplicada, IMECC-UNICAMP, C.P. 6065, 13083-859 Campinas, SP, Brazil.

We reexamine here a problem considered in detail before by Waugh and Lake: the solution of spherically symmetric Einstein's equations with a radial flow of unpolarized radiation (the Vaidya metric) in double-null coordinates. This problem is known to be not analytically solvable; the only known explicit solutions correspond to the constant mass case (Schwarzschild solution in Kruskal-Szekeres form) and the linear and exponential mass functions originally discovered by Waugh and Lake. We present here a semianalytical approach that can be used to discuss some qualitative and quantitative aspects of the Vaidya metric in double-null coordinates for generic mass functions. We present also a new analytical solution corresponding to $(1/v)$-mass function and discuss some physical examples.

I. INTRODUCTION

The Vaidya metric [1], which in radiation coordinates (w, r, θ, ϕ) has the form

$$ds^2 = -\left(1 - \frac{2m(w)}{r}\right)dw^2 + 2c\,dr\,dw + r^2 d\Omega^2, \quad (1)$$

where $d\Omega^2 = d\theta^2 + \sin^2\theta d\phi^2$, $c = \pm 1$, is a solution of Einstein's equations with spherical symmetry in the eikonal approximation to a radial flow of unpolarized radiation. For the case of an ingoing radial flow, $c = 1$ and $m(w)$ is a monotone increasing mass function in the advanced time w, while $c = -1$ corresponds to an outgoing radial flow, with $m(w)$ being in this case a monotone decreasing mass function in the retarded time w. For many years, it has been used in the analysis of spherical collapse and the formation of naked singularities (For references, see the extensive list of [2] and also [3]). It is known that Vaidya metric can be obtained, by taking appropriate limits in the self-similar case, from the Tolman metric representing spherically symmetric dust distribution [4]. This result has shed some light on the nature of the so-called shell-focusing singularities [5], discussed in details in [2,6–8]. The Vaidya metric has also proved to be useful in the study of Hawking radiation and the process of black-hole evaporation[9–13], and more recently, in the stochastic gravity program[14].

Motivated by the long-known fact that the radiation coordinates are defective at the horizon [15], implying that the Vaidya metric (1) is not geodesically complete (see [16] for considerations about possible analytical extensions), Waugh and Lake [17] considered the problem of casting the Vaidya metric in double-null coordinates (u, v, θ, ϕ). As all previous attempts to construct a general transformation from radiation to double-null coor-

dinates have failed, they followed Synge [18] and considered Einstein's equation with spherical symmetry in double-null coordinates *ab initio*. The spherically symmetric line element in double-null coordinates is

$$ds^2 = -2f(u, v)du\,dv + r^2(u, v)d\Omega^2, \quad (2)$$

where $f(u, v)$ and $r(u, v)$ are nonvanishing functions. The energy-momentum tensor of a unidirectional radial flow of unpolarized radiation in the eikonal approximation is given by

$$T_{ab} = \frac{1}{8\pi} h(u, v) k_a k_b, \quad (3)$$

where k_a is a radial null vector. As Waugh and Lake, we will consider, without loss of generality, the case of the flow along v-direction: $k_a = (0, 1, 0, 0)$. The case of simultaneous ingoing and outgoing flows was considered in [19]. Einstein's equations are less constrained in such case, allowing the construction of some similarity solutions. In our case, the metric (2) with the energy-momentum tensor (3) reduce to the following set of equations [17]:

$$f(u, v) = 2B(v)\partial_u r(u, v), \quad (4)$$

$$\partial_v r(u, v) = -B(v)\left(1 - \frac{2A(v)}{r(u, v)}\right), \quad (5)$$

$$h(u, v) = -4\frac{B(v)A'(v)}{r^2(u, v)}, \quad (6)$$

where $B(v)$ and $A(v)$ are arbitrary functions obeying, according to the weak energy condition,

$$B(v)A'(v) \leq 0. \quad (7)$$

Note that from (4), the regularity of $f(u, v)$ requires $B(v) \neq 0$. Schwarzschild solution in the Kruskal-

*Electronic address: asaa@ime.unicamp.br

    70 084014-1

Szekeres form corresponds to $A' = 0$. For $A' \neq 0$, the choice

$$2B(v) = -\frac{A'}{|A'|} \tag{8}$$

allows one to interpret $A(v)$ as the mass of the solution and v as the proper time as measured in the rest frame at infinity for the asymptotically flat case [17]. We assume here $A(v) > 0$. The radial flow is ingoing if $A' > 0$, and outgoing if $A' < 0$. Note that if the weak energy condition (7) holds, the function $A(v)$ is monotone, implying that the radial flow must be ingoing or outgoing for all v. It is not possible, for instance, to have "oscillating" mass functions $A(v)$ in double-null coordinates.

The problem may be stated in the following way: given the functions $A(v)$ and $B(v)$, Eq. (5) shall be integrated and $r(u, v)$ is obtained. Then, $f(u, v)$ and $h(u, v)$ are calculated from (4) and (6). The arbitrary function of u appearing in the integration of (5) must be chosen properly to have a nonvanishing $f(u, v)$ function from (4). Unfortunately, this procedure is not analytically solvable in general. Waugh and Lake, nevertheless, were able to find regular solutions for Eqs. (4)–(6) for linear [$A(v) = \lambda c v$] and a certain exponential $\{A(v) = \frac{1}{\beta}[\alpha \exp(\beta c v/2) + 1]\}$ mass functions (λ, α, and β are positive constants, $c = \pm 1$, corresponding to ingoing/outgoing flow, respectively). To the best of our knowledge, these are the only varying mass analytical solutions obtained in double-null coordinates so far. We notice, however, that Kuroda was able to construct a transformation from radiation to double-null coordinates for some particular mass functions [10,11].

In the following section, we will present a semianalytical approach to attack the problem of solving Eqs. (4)–(6) for general mass functions obeying the weak energy condition (7). The approach allows us to construct qualitatively conformal diagrams, identifying horizons and singularities, and also to evaluate specific geometric quantities. Before, however, we notice that one can solve analytically Eqs. (4)–(6) also for the case of

$$A(v) = \frac{\kappa^2}{v}, \tag{9}$$

being κ a massive parameter, and $B = 1/2$. With the mass function (9), Eq. (5) can be integrated as

$$L(r, u, v) = P(u)v + 2\kappa e^{\xi^2} - \sqrt{2}v \int_0^\xi e^{s^2} ds = 0, \tag{10}$$

where

$$\xi = \frac{1}{2\sqrt{2}}\left(\frac{v}{\kappa} + 2\frac{r}{\kappa}\right) \tag{11}$$

and $P(u)$ is an arbitrary function. It is quite easy to show that $L(r, u, v) = 0$ is an invariant surface of (5), i.e, one has

$$\frac{dL}{dv} = \frac{\partial L}{\partial r}\partial_v r + \frac{\partial L}{\partial v} = \frac{1}{v}L \tag{12}$$

along the solutions of (5). From (4), we have

$$f = -\kappa P'(u)v\frac{e^{-\xi^2}}{2r}. \tag{13}$$

The function $P(u)$ must be chosen to preclude zeros of $f(u, v)$. With $P(u) = -u/\kappa$, we have from (10)

$$\frac{u}{\kappa}\frac{v}{\kappa} = 2e^{\xi^2} - \sqrt{2}\frac{v}{\kappa}\int_0^\xi e^{s^2} ds. \tag{14}$$

Equation (14) defines $r(u, v)$. Its graphics and the corresponding conformal diagram are presented in Fig. 1.

The only spacetime singularity for $v > 0$ is $r = 0$. We recall that the Kretschmann scalar for metrics of the form (2) obeying (4)–(6) is given by [17]

$$K = R_{abcd}R^{abcd} = 48\frac{A^2(v)}{r^6}. \tag{15}$$

The resulting spacetime corresponds to a naked singularity that vanishes smoothly, giving rise to an empty spacetime. Its causal structure is identical to the first linear case ($\lambda > 1/16$) of Waugh and Lake, with time reversed (see below).

We finish this section noticing that algebraic manipulation programs (Maple, for instance) are able to find solutions of (5) for the case $A(v) \propto v^2$ in terms of Airy functions, but they seem too cumbersome to be useful. Furthermore, their causal structure is always similar to the ($\lambda > 1/16$) linear case of Waugh and Lake. Also, Kuroda has considered before the case of $M(w) = \mu w^n$
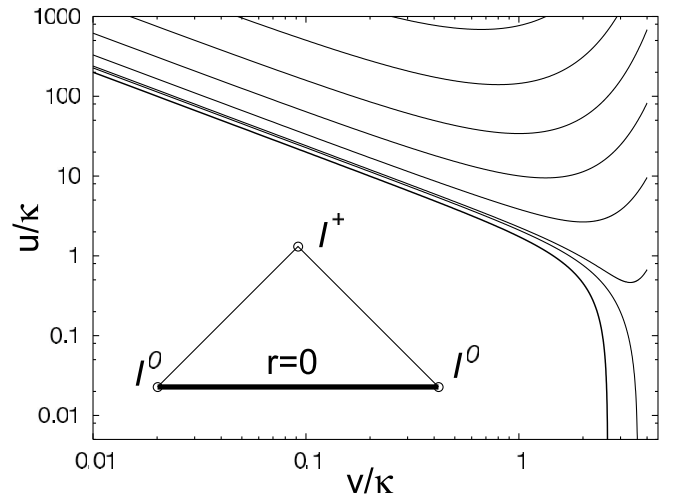

FIG. 1. Constant r/κ curves for the case $A(v) = \kappa^2/v$. The values of r/κ shown are, from bottom to top, 0, 0.5, 0.6, 1, 1.5, 2, 2.5 and 3. Future is to right and up. The corresponding conformal diagram is inserted. Here, $r = 0$ is a naked singularity.

for small w and $n \geq 1$ in radiation coordinates, obtaining some local properties of the singularity $r = w = 0$ [11].

II. SEMIANALYTICAL APPROACH

Equation (5) along u constant is a first order ordinary differential equation in v. One can evaluate the function $r(u, v)$ in any point by solving the v-initial-value problem knowing $r(u, 0)$. The trivial example of Minkowski spacetime ($A = 0$), for instance, can be obtained by choosing $r(u, 0) = u/2$.

The curve $r = 2A(v)$ is the frontier of two regions of the (v, r) plane where the solutions of (5) have qualitative distinct behaviors. Suppose, for instance, $A'(v) > 0$ (and $B = -1/2$. The case of an outgoing radiation flow follows in a straightforward manner). For all points of the plane (v, r) below this curve, $r' < 0$ (See Fig. 2). Hence, any solution entering in this region will, unavoidably, reach the singularity at $r = 0$, with finite v. Suppose a given solution $r_i(v)$ with initial condition $r_i(0) = r_i$ enters into this region. As the uniqueness of solutions for (5) is guaranteed for any point with $r \neq 0$, solutions never cross each other in the plane (v, r) for $r \neq 0$. Hence, any solution starting at $r(0) < r_i$ is confined to the region below $r_i(v)$, and it will also reach the singularity at $r = 0$ with finite v. On the other hand, suppose that a given solution $r_e(v)$ with initial condition $r_e(0) = r_e$ never enters into the region below the curve $r = 2A(v)$. Any solution starting at $r(0) > r_e$ is, therefore, confined to the region above
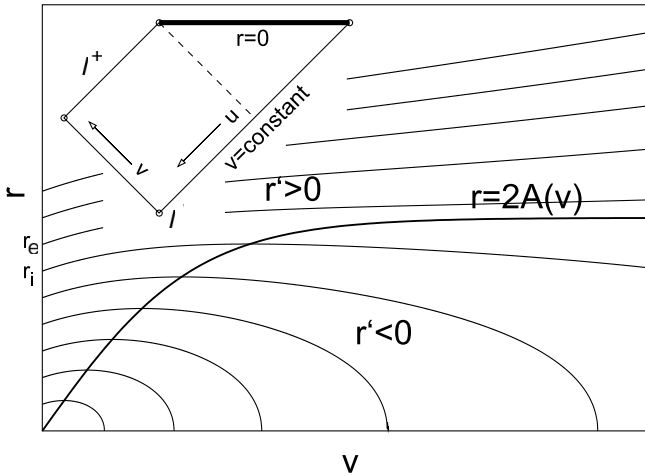

FIG. 2. In the region below the generic monotonic function $r = 2A(v)$ (the apparent horizon), all solutions have $r' < 0$. Any solution that enters into this region will reach the singularity at $r = 0$ with finite v. On the other hand, solutions confined to the $r' > 0$ region always escape from the singularity and reach $\mathcal{I}^+$. In this case, supposing that the mass function $A(v)$ has an asymptotic value such that $r_i(v) < 2A(v) < r_i(v)$, there exists an event horizon (the dashed line on the conformal diagram) somewhere between the solutions $r_i(v)$ and $r_e(v)$. The vector $T = \partial_v - \partial_u$ points to the future for the ingoing radiation case.

$r_e(v)$ and will escape from the singularity at $r = 0$. Keeping in mind that these solutions correspond to null trajectories with u constant, it is possible to infer the causal structure of the spacetime from their qualitative behavior and an appropriate choice for the initial conditions $r(u, 0)$. For instance, in the case of Fig. 2, supposing that the mass function $A(v)$ has an asymptotic value such that $r_i(v) < 2A(v) < r_i(v)$, an event horizon shall be located somewhere between $r_i(v)$ and $r_e(v)$.

Event horizons are global structures. One needs to know the total ($v \to \infty$) spacetime evolution to define them. On the other hand, apparent horizons are defined locally [20]. Indeed, they are the real relevant ones in our semianalytical approach. The curve $r = 2A(v)$ is an apparent horizon. For a given v, all solutions in Fig. 2 such that $r(v) \leq 2A(v)$ will be captured by the singularity. Solutions for which $r(v) > 2A(v)$ are temporally free, but they may find themselves trapped later if $A(v)$ increases. The event horizon is the last of these solutions trapped by the singularity.

We remind that Eq. (4) requires that $\partial_u r(u, v) \neq 0$, implying that, for v constant, $r(u + du, v) \neq r(u, v)$ for all u. This condition holds everywhere we have uniqueness of the solutions of (5), provided that the initial conditions are such that $\partial_u r(u, 0) \neq 0$. Moreover, if $\partial_u r(u, 0) > 0$, then $\partial_u r(u, v) > 0$, implying from (4) that the sign of $f(u, v)$ will be determined by $B(v)$. For the ingoing radiation case, one has $B(v) = -1/2$, and from (2) one sees that the vector field $T = \partial_v - \partial_u$ is timelike. Our conformal diagrams are oriented such that this vector field points upward. If the condition $\partial_u r(u, 0) \neq 0$ holds, the conformal diagrams obtained for a given $A(v)$ from different initial conditions are always equivalent. Some explicit examples will clarify the proposed approach.

A. Linear mass function

The linear mass function solution discovered by Waugh and Lake corresponds to $A = \lambda v$ and $B = -1/2$ (the ingoing radiation case, the outgoing one also follows in a straightforward way). Note that with these choices, Eq. (5) does not satisfy the Lipschitz condition in $r = 0$, implying that uniqueness is not guaranteed for solutions passing there. This will be a crucial point to clarify the nature of the three qualitative different cases identified by Waugh and Lake, corresponding to $\lambda > 1/16$, $\lambda = 1/16$, and $\lambda < 1/16$. We notice that the linear mass case was also considered in [8] in great detail and in a more general situation (the case of a charged radial null fluid).

The frontier of the region where all the solutions reach the singularity at $r = 0$ is, in this case, the straight line $r = 2\lambda r$. Taking the v-derivative of (5), one gets

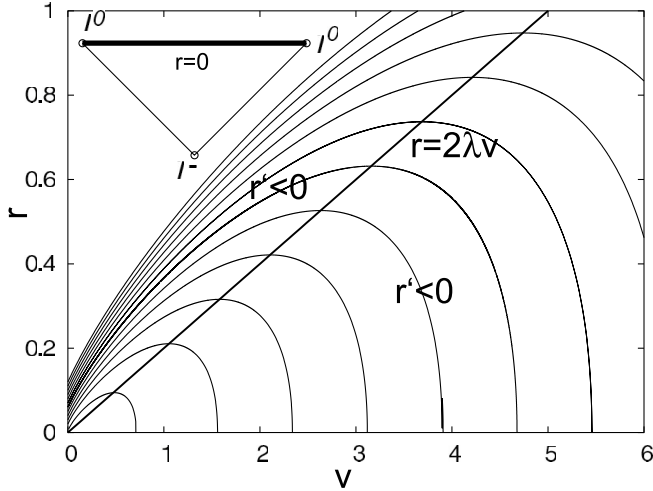$$r'' = \frac{\lambda}{r}\left[\frac{v}{2r}\left(1 - \frac{2\lambda v}{r}\right) - 1\right]. \tag{16}$$

FIG. 3.   For $\lambda > 1/16$, all solutions are concave for $v > 0$. Hence, all null trajectories along v necessarily reach the singularity at $r = 0$. The figure corresponds to the case $\lambda = 1/10$. The conformal diagram is inserted.

The regions in the plane (v, r) where the solutions obey $r'' = 0$ are the straight lines

$$r = \frac{v}{4}\left(1 \pm \sqrt{1 - 16\lambda}\right). \tag{17}$$

One can reproduce the analysis of Waugh and Lake for the three qualitative different cases according to the value of λ by considering the possible solutions of (17). For this purpose, we will consider the solutions of (5) with the initial condition $r(u, 0) \propto u$.

For $\lambda > 1/16$, the case showed in Fig. 3, $r'' < 0$ for all points with $v > 0$, and the only relevant frontier is the $r = 2\lambda v$ straight line (the apparent horizon). All solutions of (5) are concave functions and cross the $r' = 0$ line, reaching the singularity with a finite v which increases monotonically with u. The causal structure of the corresponding spacetime is very simple. There is no horizon, and the future cone of all points ends in the singularity at $r = 0$.

Each curve in Fig. 3 corresponds to a constant u slice of the full solution $r(u, v)$. It is possible, in principle, to reconstruct the two dimensional surface $r(u, v)$ and to plot its lines of constant r on the (u, v) plane, as done in Fig. 1, reproducing all original results of Waugh and Lake [17]. However, these lines are not necessary to construct the conformal diagrams.

For $\lambda = 1/16$, $r'' = 0$ on the line $r = v/4$. This straight line itself is a solution. All other solutions are concave functions. We have two distinct qualitative behaviors for the null trajectories along u constant. All solutions starting at $r(0) > 0$ are confined to the region above $r = v/4$. They never reach the singularity, all trajectories reach I^+. However, in the region below $r = v/4$, we have infinitely many concave trajectories starting and ending
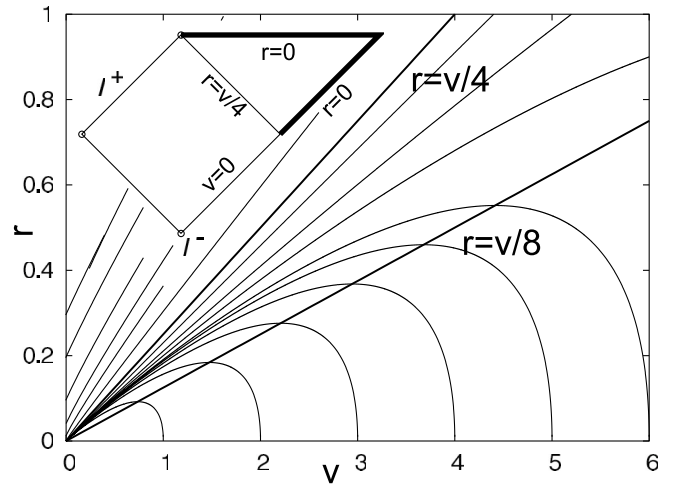

FIG. 4.   For $\lambda = 1/16$, we have two relevant lines in the (r, v) plane: $r = v/4$ and $r = v/8$. The first one plays the role of an event horizon, separating the two regions of distinct qualitative behavior for the null trajectories along v. Beyond the horizon, all solutions escape to infinity. Inside, all solutions reach the singularity $r = 0$ with finite v. The conformal diagram is inserted. The singularity at $r = 0$ is a shell-focusing one.

in the (shell-focusing) singularity. They start at $r(0) = 0$, increase in the region between $r = v/4$ and $r = v/8$, cross the last line and reach unavoidably $r = 0$ again, with finite v. The trajectory $r = v/4$ plays the role of an event horizon, separating two regions with distinct qualitative behavior: one where constant u null trajectories reach I^+ and another where they start and end in the singularity. This situation is shown in Fig. 4. This behavior is only possible, of course, because the solutions of (5) fail to be unique at $r = 0$.

For $\lambda < 1/16$ (Fig. 5), we have three distinct regions according to the concavity of the solutions. They are limited by the two straight lines (17) that are also solutions of (5). Between them, solutions are convex. Above r_+ and below r_-, solutions are concave. The last line is the inner horizon. Inside, the null trajectories with constant u start and end in the singularity $r = 0$. The line r_+ is an outer horizon. Between them, the constant u null trajectories start in the naked singularity and reach I^+. Beyond the outer horizon, all constant u null trajectories escape the singularity.

B. Collapse of a radial null fluid

As an example of the proposed approach applied to new mass functions, let us consider first the case of a collapse of incoming radial null fluid, starting with the empty space. This could be described, for instance, by the mass function
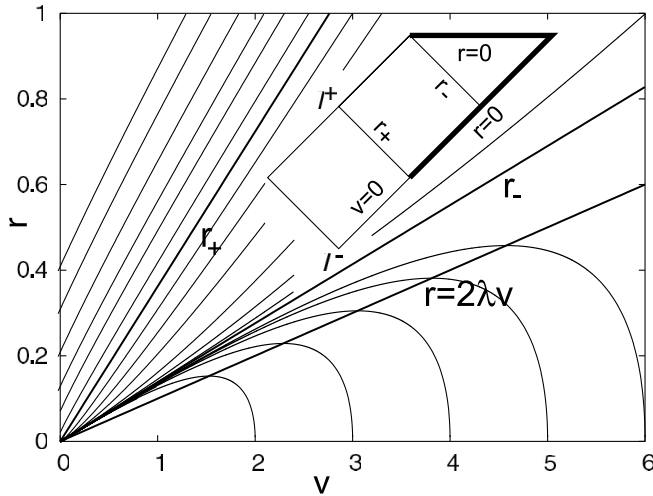
$$A(v) = \frac{m}{2}(1 + \tanh\rho v). \tag{18}$$

FIG. 5.   With $\lambda < 1/16$, we have two horizons r_- and r_+. Any solution starting above r_+ always escapes to I_+. Solutions starting inside the inner event horizon r_i always reach the singularity at $r = 0$. Between the horizons, solutions start in the naked singularity but escape to I_+. The figure corresponds to the case $\lambda = 1/20$. The conformal diagram is inserted.

The corresponding spacetime is empty for $v \to -\infty$, it receives smoothly a radial flow of null fluid, and finishes as a black hole of mass m for $v \to \infty$. The solutions of (5) are presented in the Fig. 6. With the mass function (18), we always have a singularity at $r = 0$ for $v \neq -\infty$. The constant u null trajectories approach $r = 0$ asymptotically for $v \to -\infty$. Some of them, confined by the horizon, are captured by the collapse and reach the singularity, and others escape to $I +$. Any initial condi-
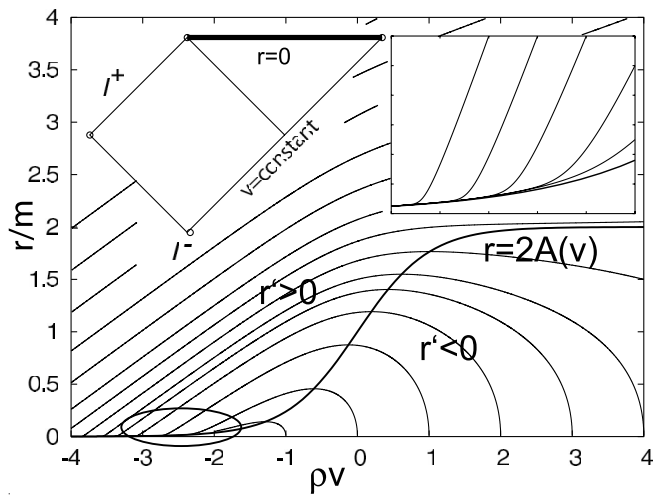
tion obeying $\partial_u r(u, v_0) \neq 0$ leads to the same causal structure.

The proposed semianalytical procedure can be used also to derive some qualitative results. One could, for instance, locate accurately the event horizon in this case. Since we do not expect deviations from the Minkowski spacetime for $v \to -\infty$, we could start with initial conditions such that $r(u, -\infty) = u/2$. Then, we identity in the solutions of (6) the one [the horizon $r_h(v)$)] approaching asymptotically the curve $r = 2A(v)$ for large v. For large values of v_0, the horizon would be located at $[2r_h(-v_0), -v_0]$.

C. Black-hole evaporation

As a last example, let us consider the physically relevant case of black-hole evaporation. We remind that much work has been devoted on Vaidya metric to describe black-hole evaporation[9–13]. Our approach allows us to analyze this question in the more convenient double-null coordinates. The process of black-hole evaporation supposes $A' < 0$ and an outgoing radiation flow. Hence, one needs to chose $B(v) = 1/2$ in our procedure. With this choice, we see from (4) that $f(u, v) > 0$, implying that the field $\partial_v - \partial_u$ is not timelike anymore. It is, namely, its orthogonal vector field $\partial_v + \partial_u$ that will define the time

FIG. 6.   The case $A(v) = m(1 + \tanh\rho v)/2$. The solutions tend asymptotically to $r = 0$ when $v \to -\infty$. A zoom of the range $-3 < v < -2$ illustrating such asymptotic behavior is inserted. In this case, $r = 0$ is always singular for $v > -\infty$. This plot corresponds to $m\rho = 1$; the situation is qualitatively identical for other cases. The conformal diagram is inserted.
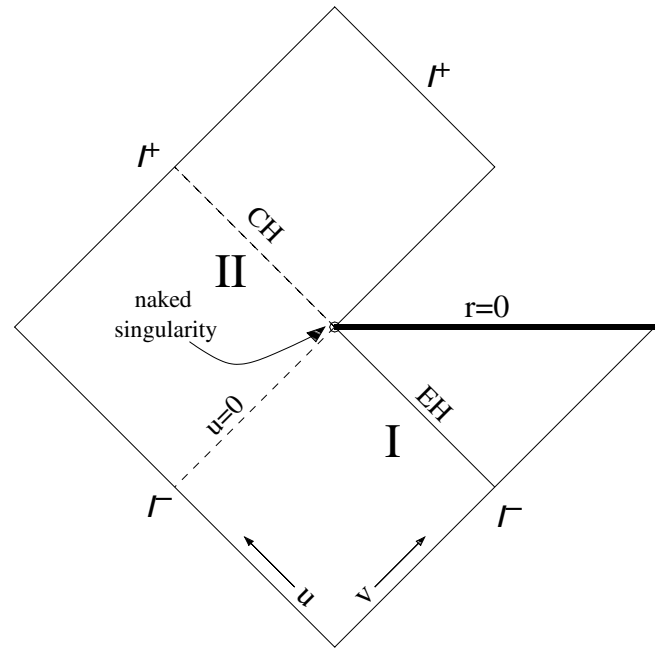

FIG. 7.   Conformal diagram for an evaporating black hole with mass $A(u)$ given by (21). The region I corresponds to the black hole, and can be obtained, by using the transformations (19), from the ingoing radiation case. Region II is the empty space left after the vanishing of the black hole at $u = 0$. The event horizon is the line EH. The dashed CH line is a Cauchy horizon. Beyond it, we have breakdown of predictability due to the naked singularity left by the black hole.

evolution in this case. In order to keep the future direction pointing upward in the conformal diagrams, one needs to reorient the coordinates u and v. The appropriate transformation here is

$$v \to u, \qquad u \to -v. \qquad (19)$$

With this choice and $B(v) = 1/2$, Eq. (5) reads

$$\partial_u r(u, v) = \frac{1}{2}\left(1 - \frac{2A(-u)}{r(u, v)}\right), \qquad (20)$$

which is formally identical to the equation for the ingoing case characterized by the mass function $A(-u)$ with radiation flow along the u direction. Hence, the description of an outgoing situation with decreasing mass function $A(u)$ can be obtained by applying the transformation (19) for the ingoing case corresponding to the mass function $A(-v)$.

With the help of (19), one could construct the conformal diagram corresponding to the mass function $A(u) = m(1 - \tanh\rho u)/2$ starting from the last example. Such a case, however, does not correspond really to an evaporating black hole since, according to this mass function, the black hole never disappears, the singularity at $r = 0$ is ever present for $u < \infty$. In a real process of black-hole evaporation due to Hawking radiation, the black hole loses mass with a rate $\dot{M} \propto M^{-2}$, disappearing completely in a finite time and giving rise to an empty spacetime. The mass function

$$A(u) = \begin{cases} -m \tanh\rho u, & u < 0, \\ 0 & u \geq 0, \end{cases} \qquad (21)$$

can be used to simulate the vanishing of a black hole in a finite time. For the ingoing radiation case $A(-v)$, the situation is similar to the last example, but with the crucial difference that for $v \leq 0$ the spacetime is empty, and the solutions can reach (and cross) $r = 0$. We notice that the form of $A(u)$ is not important. In order to construct the conformal diagram of an evaporating black

hole, one only needs that $A(u) = 0$ after some $u < \infty$. In this case, the full conformal diagram (see Fig. 7) is constructed adding to that one obtained from the ingoing collapse case by using the transformation (19), a patch of Minkowski spacetime, just after the instant $u = 0$ corresponding to the vanishing of the black hole. The resulting conformal diagram represents a black hole that evaporates leaving behind a naked singularity.

III. CONCLUSION

We presented a semianalytical approach to construct the Vaidya metric in double-null coordinates for general monotonic mass functions. We applied it to elucidate the nature of the three distinct qualitative causal structures identified by Waugh and Lake [17] for linear mass functions, to construct a solution corresponding to a smooth radial collapse of a null fluid, starting from empty space and finishing with a black hole, and to construct the conformal diagram of an evaporating black hole.

The approach involves an arbitrary function $r(u, 0)$. However, any choice for which $\partial_u r(u, 0) \neq 0$ will result in causally equivalent regular $[f(u, v) \neq 0]$ spacetimes. The analytical solutions of this problem also involve an arbitrary function, as $P(u)$ in (10), that must be chosen properly in order to get a regular spacetime.

The double-null form of the Vaidya metric is suitable to the study of quasinormal modes of time-dependent solutions. In double-null coordinates, the equations for scalar perturbations are separable and we obtain an effective Schrödinger equation with a time-dependent potential for the perturbations. This situation has been recently considered in the heuristic analysis of [21]. The full problem is now under investigation.

[1] H. Stephani *et al.*, *Exact Solutions of Einstein's Field Equations* (Cambridge University Press, Cambridge, England, 2002).
[2] K. Lake, Phys. Rev. Lett. **68**, 3129 (1992).
[3] P. S. Joshi, *Global Aspects in Gravitation and Cosmology* (Oxford University, New York, 1993).
[4] J. P. S. Lemos, Phys. Rev. Lett. **68**, 1447 (1992); C. Hellaby, Phys. Rev. D **49**, 6484 (1994).
[5] D. M. Eardley and L. Smarr, Phys. Rev. D **19**, 2239 (1979).
[6] Y. Kuroda, Prog. Theor. Phys. **72**, 63 (1984).
[7] K. Lake and T. Zannias, Phys. Rev. D **41**, 3866 (1990).
[8] K. Lake and T. Zannias, Phys. Rev. D **43**, 1798 (1991).
[9] W. A. Hiscock, Phys. Rev. D **23**, 2813 (1981).
[10] Y. Kuroda, Prog. Theor. Phys. **71**, 100 (1984).
[11] Y. Kuroda, Prog. Theor. Phys. **71**, 1422 (1984).
[12] W. Biernacki, Phys. Rev. D **41**, 1356 (1990).
[13] R. Parentani, Phys. Rev. D **63**, 041503 (2001).
[14] B.-L. Hu and E. Verdaguer, Living Rev. Relativity **7**, 3 (2004).
[15] R. Lindquist, R. Schwartz, and C. Misner, Phys. Rev. **137**, B1364 (1965).
[16] F. Fayos, M. M. Martin-Prats, and J. M. M. Senovilla, Classical Quantum Gravity **12**, 2565 (1993).
[17] B. Waugh and K. Lake, Phys. Rev. D **34**, 2978 (1986).

[18] J. Synge, Annali di matematica pura ed applicata **98**, 239 (1974).

[19] P. R. Holvorcem, P. S. Letelier, and A. Wang, J. Math. Phys. (N.Y.) **36**, 3663 (1995).

[20] S. W. Hawking and G. F. Ellis, *The Large Scale Structure of Space-Time* (Cambridge University Press, Cambridge, England, 1973).

[21] S. Hod, Phys. Rev. D **66**, 024001 (2002).